First-principles study of the interaction between paramagnetic V^{4+} centers through formally magnetically inactive VO_4 tetrahedra in the quasi-one-dimensional spin systems $Sr_2V_3O_9$ and $Ba_2V_3O_9$

Antonio Rodríguez-Fortea,[1] Miquel Llunell,[2] Pere Alemany,[2] and Enric Canadell[3]
[1]*Departament de Química Física i Inorgànica, Universitat Rovira i Virgili, Marcel.lí Domingo s/n, 43007 Tarragona, Spain*
[2]*Departament de Química Física i Institut de Química Teòrica i Computacional (IQTCUB), Universitat de Barcelona, Diagonal 647, 08028 Barcelona, Spain*
[3]*Institut de Ciència de Materials de Barcelona, CSIC, Campus UAB, 08193 Bellaterra, Spain*
(Received 20 May 2010; revised manuscript received 20 September 2010; published 11 October 2010)

We report a first-principles density-functional theory study of the origin of the magnetic properties of the quasi-one-dimensional spin systems $Sr_2V_3O_9$ and $Ba_2V_3O_9$. The calculated coupling constants are in very good agreement with experimental data and provide a basis to understand the correlation between structural features and magnetic coupling constants. In $Sr_2V_3O_9$, the predominant coupling is antiferromagnetic and is indeed mediated by one of the two different types of VO_4 tetrahedra. However, there is also a weaker ferromagnetic interaction along the direction of the octahedral chains, which is mediated by the corner-sharing oxygen atoms through a spin-polarization mechanism. The second type of tetrahedra apparently do not contribute to the magnetic coupling. In $Ba_2V_3O_9$, the antiferromagnetic coupling is dominated by a very substantial superexchange interaction of the vanadium d_{xy} orbitals through the tetrahedra sharing only one oxygen atom with the octahedral chain. The second type of tetrahedra and the oxygen atoms nonshared with the tetrahedra provide ferromagnetic interactions which only partially counteract the antiferromagnetic superexchange coupling. Interchain disorder is predicted to have a very small influence on the coupling constants.

DOI: 10.1103/PhysRevB.82.134416 PACS number(s): 71.70.Gm, 71.70.Ch, 75.50.Ee, 71.20.Ps

I. INTRODUCTION

Vanadium bronzes have a rich structural chemistry exhibiting remarkable diversity in their physical properties. For instance, the tunnel-like framework of V_2O_5 allows the intercalation of numerous guest species and many phases exhibiting intriguing conducting and magnetic properties have been reported. α'-NaV_2O_5 (Ref. 1) and β-$Na_{1/3}V_2O_5$ (Ref. 2) rank among the better known materials of this family. The first is a quarter-filled spin ladder which was initially thought to be a spin-Peierls system[3] but later was shown to undergo a charge-ordering transition.[4] The second is a metal undergoing a metal-insulator transition[5] and exhibiting superconductivity under high pressure.[6] Even staying within the sodium-vanadium-oxygen phase diagram, other materials with different structures and remarkable physical properties have been reported. Worthy of note are $Na_2V_3O_7$,[7] a nanotubular phase with a complex interplay of different exchange interactions,[8–10] $Sr_2V_3O_9$,[11,12] a quasi-one-dimensional spin system with antiferromagnetic ordering at low temperature,[13] or η-$Na_9V_{14}O_{35}$,[14,15] a spin-gap system undergoing a charge ordering transition around 100 K.[16]

The magnetic properties of most of these vanadium bronzes can usually be understood by taking into account the direct V-V interactions and/or the superexchange interactions mediated by the oxygen atoms shared by the V-centered polyhedra. However, it has been recently shown that this may not be so in phases such as $Sr_2V_3O_9$, $Ba_2V_3O_9$, or η-$Na_9V_{14}O_{35}$. Here, formally magnetically inactive $V^{5+}O_4$ tetrahedra apparently play a crucial role in leading to the observed magnetic properties. Such a strong exchange coupling between two relatively distant paramagnetic $V^{4+}(d^1)$ centers through $V^{5+}O_4(d^0)$ tetrahedra has been called superexchange (SSE) by Koo and Whangbo.[17] This is an unexpected feature which, because of its somewhat counter intuitive nature, needs to be better understood. These interactions could have been overlooked in other structures and yet play an important role. Consequently, it would be useful to have some intuitive guidelines to guess when such units can be important to be taken into account.

$Sr_2V_3O_9$ and $Ba_2V_3O_9$ are excellent candidates for such a study, a necessary prelude to the analysis of structurally more complex materials like η-$Na_9V_{14}O_{35}$. The magnetic properties of these chains were initially studied by Mentré, Steifink, and co-workers[12,18,19] and later considered in more detail by Kaul, Geibel, and co-workers[13,20–22] and others.[14,23] It is now clear that both compounds can be described as containing $S=1/2$ antiferromagnetic chains. In $Sr_2V_3O_9$, the antiferromagnetic ordering occurs at $T_N=5.3$ K indicating a weak interchain exchange. In contrast, in $Ba_2V_3O_9$ no evidence for magnetic order at low temperature was found, suggesting an even weaker interchain coupling.

Koo and Whangbo reported a dimer splitting study of these phases based on extended Hückel-type calculations[17] predicting a different origin of exchange interactions in the two compounds, with SSE being crucial in $Sr_2V_3O_9$. Nevertheless, because of the bold approximations involved in the extended Hückel method, especially in the case of a problem strongly related to the electronic repulsions which are not explicitly treated in this method, caution is needed in taking these calculations as a firm basis for understanding the magnetic properties of these materials. In addition, this type of approach can only provide an approximation to the antiferromagnetic interactions of the material,[24] a limitation that is very severe for complex systems with several mutually interacting paramagnetic centers. Kaul and co-workers[13] reported

band-structure calculations for the two systems which clarified the quasi-one-dimensional nature of the magnetic interactions and made a crude evaluation of the magnetic couplings. However, the detailed nature of the different magnetic interactions and its relationship with the structural features of the two solids has not yet been discussed in detail in the literature on the basis of accurate first-principles calculations providing a reliable estimation of their magnitude.

Here we report a first-principles study of the two materials, present reliable values for the different magnetic interactions and provide simple guidelines to understand when such $V(d^1)$-$V(d^1)$ interactions through usually magnetically inactive $V^{5+}O_4$ tetrahedra may be important.

II. COMPUTATIONAL DETAILS

First-principles spin-polarized calculations for $Sr_2V_3O_9$ and $Ba_2V_3O_9$ were carried out using a numerical atomic orbitals density-functional theory (DFT) approach[25,26] developed for efficient calculations in large systems and implemented in the SIESTA code.[27–29] We have used the generalized gradient approximation (GGA) to DFT and, in particular, the functional of Perdew, Burke, and Ernzerhof.[30] Only the valence electrons are considered in the calculation, with the core being replaced by norm-conserving scalar relativistic pseudopotentials[31] factorized in the Kleinman-Bylander form.[32] Nonlinear partial core corrections to describe the exchange and correlations in the core region were used for V.[33] We have used a split-valence triple-ζ basis set including polarization orbitals for V and O as obtained with an energy shift of 50 meV.[34] A split-valence double-ζ basis set including polarization orbitals was used for Sr and Ba; the 4*s*, 4*p*, and 4*d* electrons of Sr as well as the 5*p* and 5*d* electrons of Ba were treated as valence electrons. The energy cutoff of the real-space integration mesh was 200 Ry and the Brillouin zone was sampled using grids of $(3\times2\times3)$ and $(3\times3\times3)$ *k* points[35] for $Sr_2V_3O_9$ and $Ba_2V_3O_9$, respectively. Ordered models based on the experimental crystal structures,[12,18] as explained below, were used in the periodic calculations. The coupling constants were calculated according to the procedure described by Ruiz, Llunell, and Alemany.[36]

The DFT spin-polarized calculations for discrete molecular units were carried out adopting the hybrid B3LYP functional,[37] which has given excellent results for the calculation of magnetic coupling constants for molecular systems,[38,39] including those containing $V(d^1)$.[40] Basis sets of triple-ζ quality[41] for V and double-ζ quality for oxygen and hydrogen atoms were used. The calculations were carried out using the GAUSSIAN 03 code.[42] The geometries are the same employed for the periodic calculations and the O-H distances used for H atoms saturating the O atoms in the finite clusters were 0.96 Å for water ligands and 0.85 Å for hydroxyl ligands.

The spin Hamiltonian for a general polynuclear compound without anisotropic terms can be expressed as

$$\hat{H} = -\sum_{i,j} J_{ij}\hat{\mathbf{S}}_i \cdot \hat{\mathbf{S}}_j, \tag{1}$$

where $\hat{\mathbf{S}}_i$ and $\hat{\mathbf{S}}_j$ are the spin operators of the paramagnetic centers *i* and *j* and the J_{ij} parameters are the exchange coupling constants for all different pairwise interactions between the paramagnetic centers of the compound. For dinuclear compounds, it has been found that, when using DFT-based wave functions, reasonable estimates of the exchange coupling constants can be obtained from the energy difference between the low-spin configuration, E_{LS} (the traditionally called broken-symmetry solution for symmetric complexes), and the configuration with the highest spin, E_{HS}, by means of the following equation:[43]

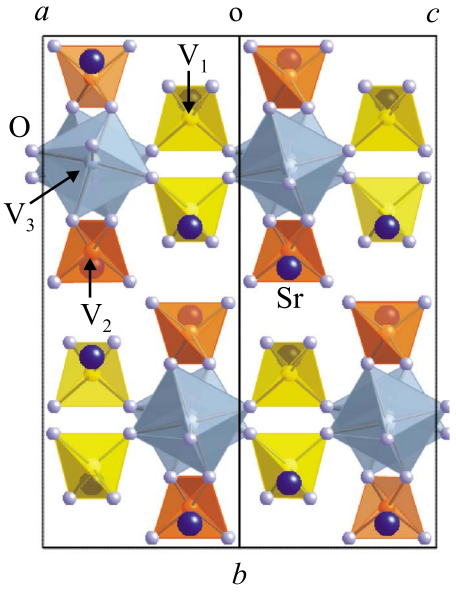

FIG. 1. (Color online) View of the crystal structure of $Sr_2V_3O_9$ along the direction of the octahedral chains. The polyhedra for the three different types of vanadium atoms are shown in different color.

$$J = \frac{E_{LS} - E_{HS}}{2S_1S_2 + S_2}, \tag{2}$$

where S_1 and S_2 are the values of the spin for the paramagnetic centers. This solution, in which the energy of the single-determinant low-spin wave function is assumed to be the energy of the low-spin state, usually provides results in agreement with experiment.[38–40] This expression can be easily extended to polynuclear and multidimensional systems.[36,43]

III. CRYSTAL STRUCTURES

To analyze the different magnetic coupling constants of $Sr_2V_3O_9$ and $Ba_2V_3O_9$, it is essential to clearly understand the details of their structures. The crystal structures of $Sr_2V_3O_9$ and $Ba_2V_3O_9$ were initially solved by Feldmann and Müller-Buschbaum[11,44] and later confirmed by Steifink and co-workers.[12,18] As shown in Figs. 1 and 2, they are both built from the condensation of VO_6 octahedra and VO_4 tetrahedra. However, there are two important differences between the two systems. First, $Sr_2V_3O_9$ is structurally a two-dimensional system whereas $Ba_2V_3O_9$ is one-dimensional. Second, the octahedral chains in $Ba_2V_3O_9$ share opposite edges but those in $Sr_2V_3O_9$ share opposite corners.

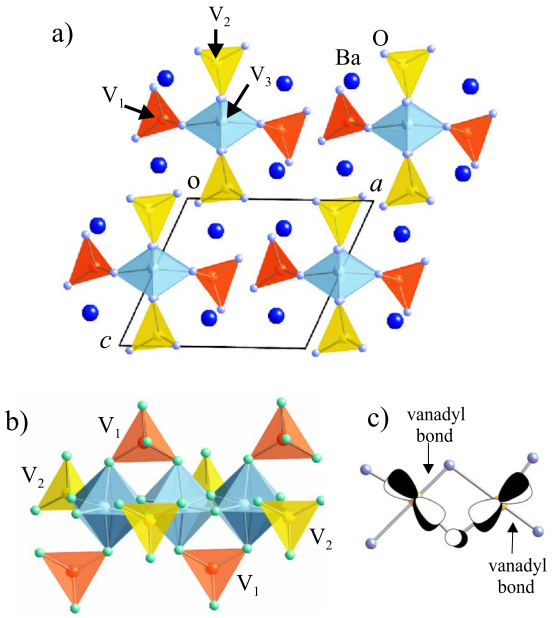

FIG. 2. (Color online) (a) View of the crystal structure of $Ba_2V_3O_9$ along the direction of the octahedral chains. (b) A different view of one octahedral chain. (c) is a top view of a fragment of the octahedral chain showing how a p orbital of one of the shared oxygen atoms can provide a significant exchange coupling along the chain.

There are two different types of tetrahedra in the two structures. In $Sr_2V_3O_9$ half of the tetrahedra share two oxygen atoms with adjacent octahedra of the chain (V_2, tetrahedra in orange) and the other half share two oxygen with two different octahedral chains (V_1, tetrahedra in yellow). Whereas the former (V_2) act as intrachain bridges, the latter (V_1) are interchain bridges, thus leading to a two-dimensional material. In $Ba_2V_3O_9$ half of the tetrahedra (V_1, tetrahedra in orange) act as intrachain bridges exactly in the same way as for $Sr_2V_3O_9$ whereas the other half (V_2) share only one oxygen with only one octahedral chain, thus leaving three oxygen unshared. This leads to the one-dimensional nature of the material. The three different vanadium atoms are labeled in Figs. 1 and 2 according to their original crystallographic description.[12,18]

An essential aspect of these structures is that the octahedra are significantly distorted with the vanadium atom displaced toward one of the oxygen atoms. This leads to the formation of a short V-O bond (≈1.7 Å, i.e., a *vanadyl bond*) and an opposite long one (≈2.2 Å). As it is well known, this feature leads to the splitting of the t_{2g} levels of the vanadium atom in a perfect octahedral environment leaving the d_{xy} orbital below the (d_{xz},d_{yz}) pair (all along our discussion we assume a local axis system such that the z direction coincides with the vanadyl bond).

In $Sr_2V_3O_9$, the octahedra are tilted with respect to the direction of the chain so that the vanadyl bonds make an angle of ~18° with the chain direction. In addition, as can be seen in Fig. 1, two successive octahedra are rotated with respect to the chain axis. The O-V-V-O dihedral angle is not far from 45° (i.e., 37.8°) and the V-V distance is relatively long (3.651 Å). Because of the different local symmetry of the vanadium d_{xy} orbital and the p orbitals of the apical oxygen atoms with respect to the O_{apical}-V-O_{apical} axis, the shared oxygen orbitals are not expected to contribute through a superexchange mechanism to the V-V coupling. Thus, the intrachain magnetic interactions involving the vanadium d_{xy} orbital are not expected to be large except if the V_2 tetrahedra play a noticeable role.

In $Ba_2V_3O_9$ the octahedra share edges [see Fig. 2(b)] and the vanadyl bonds occur in the plane containing the shared edges. Thus the vanadyl bonds make an angle of ~40.3° with the chain direction and are arranged in a zigzag way. Consequently, one of the two oxygen atoms of the shared edge makes π-type interactions with the vanadium d_{xy} orbitals of two adjacent octahedra [see Fig. 2(c)] and thus may provide a good superexchange interaction along the chain. Consequently, the two solids are expected to exhibit a different magnetic behavior.

Although the existence of the vanadyl bond is a clear-cut experimental result, the crystal structure refinements cannot clearly establish in which sense it occurs. This leads to a splitting of the vanadium site in two positions which are statistically occupied to 50%. However, on the basis of chemical wisdom as well as energy considerations (for instance, a calculation in which two vanadyl bonds implicate the same vanadium atom in the chains of $Ba_2V_3O_9$ indicates that such defect in the completely ordered chains destabilizes the system by almost 3 eV) the existence of a vanadium atom engaged into two vanadyl bonds is not realistic so that one expects a long-range order of the vanadyl bonds along *each octahedral chain*. The very small energy difference for the case where two adjacent octahedral chains exhibit in-phase or out-of-phase arrangements of vanadyl bonds (see below) makes unclear what is the full three-dimensional structure of these compounds.

IV. RESULTS AND DISCUSSION

A. Magnetic coupling in $Sr_2V_3O_9$

The octahedral chains in this material run along the $(a+c)$ direction [Fig. 3(a)]. The unit cell contains two symmetry equivalent layers and four octahedral vanadium atoms, two in each layer. Within a layer we consider two interactions [see Fig. 3(b)] characterized by their respective coupling constants J_1 and J_2. Taking into account that there are four different V^{4+} centers per unit cell, 16 different spin configurations can be generated although many of them are equivalent and only four of them are different. To ensure that our calculations are precise enough, we have calculated the total energy for all 16 possible spin configurations and verified that those which are equivalent have energies which differ by less than 1 K. To fulfill this requirement we had to lower the convergence criterion for the elements of the density matrix to 10^{-6}. From the four different spin configurations we can: (i) evaluate the total coupling constant J_1+J_2 as −110.5 K and (ii) conclude that the interlayer interactions are extremely weak (i.e., ~−0.06 K) and within the error limit of our calculations. The value for J_1+J_2 is in reasonable agreement with the experimental value of −82 K for the antiferromagnetic coupling. However, one must bear in mind

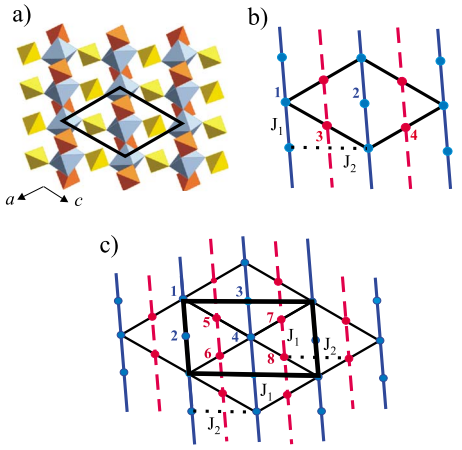

FIG. 3. (Color online) (a) View of a single layer of $Sr_2V_3O_9$; (b) schematic representation of the different octahedral chains in $Sr_2V_3O_9$. Dots refer to vanadium atoms and the solid (blue) and broken (red) lines denote chains in the upper and lower layer of the unit cell; (c) schematic view of the double cell (bold lines in black) used in the calculations.

that the experimental value was obtained by fitting the susceptibility to a one-dimensional model. The qualitative analysis given by Koo and Whangbo[17] predicts that $J_2 \gg J_1$. The difference between our calculated and the experimental values suggests however that although the SSE coupling dominates the magnetic behavior of the system, the J_1 coupling cannot be neglected. However, the topology of the lattice is such that it is not possible to obtain the separate values of the two constants using the crystallographic cell. Thus, a double cell like that schematically shown in Fig. 3(c) must be used.

Using this double cell and assuming that the interlayer couplings are nil, the J_2 and J_1 coupling constants are evaluated to be −122.6 K and +14.5 K, respectively. The calculated value of (J_1+J_2) agrees within 2 K with that obtained when using other spin configurations and with the value of the single-cell calculations as well. Thus, we confirm that $Sr_2V_3O_9$ is essentially a one-dimensional antiferromagnet along the direction of the SSE interactions although it has also a weak but non-negligible ferromagnetic interaction along the direction of the octahedral chains. These first-principles values provide support for the more crude estimation of Kaul *et al.*[13] The non-negligible, positive value obtained for J_1 evidences the shortcomings of the dimer splitting analysis based on the extended Hückel method.

Finally, we considered the possible influence of disorder on the coupling constants. As noted above, for clear-cut chemical and computational reasons the vanadyl bonds of a given chain must be ordered. In addition, the interlayer interactions are calculated to be almost negligible. Thus, only disorder within a given layer may influence the values of J_1 and J_2. We have carried out the double-layer series of calculations assuming either in-phase or out-of-phase displacements for the vanadyl bonds of the two octahedral chains in each layer. We obtain values of −122.6 K/−129.1 K and +14.5 K/+15.0 K for J_2 and J_1 in the in-phase/out-of-phase calculations, which clearly prove that disorder has a minor influence on the two coupling constants. Even if the strength of the antiferromagnetic interaction may slightly increase, the qualitative description of the magnetic interactions remains the same.

B. Magnetic coupling in $Ba_2V_3O_9$

As shown in Fig. 2, the octahedral chains in $Ba_2V_3O_9$ are not directly linked thus simplifying the calculation of the magnetic coupling constants. In this case intrachain disorder of the vanadyl bonds is also very unlikely since it would generate oxygen atoms in an unreasonable chemical environment. Thus we have adopted a model with completely ordered chains for the calculations. Single-cell calculations lead to an energy difference of 194.8 K favoring the antiferromagnetic ordering along the chain. This leads to a coupling constant of −97.4 K, in excellent agreement with the experimental value of −94 K.[13] We have also carried out a calculation using a double cell to evaluate the strength of the interchain interactions. The energy difference for the situation in which two adjacent chains have ferromagnetic or antiferromagnetic ordering is only 1.2 K per chain. Consequently, disorder cannot have any substantial influence on the magnetic coupling in this compound.

C. Structural origin of the magnetic coupling in $Sr_2V_3O_9$ and $Ba_2V_3O_9$

The calculated values of the coupling constants for both compounds are in excellent agreement with the experimental values. However, we have not yet gained a clear understanding of how these values correlate with the details of their structures. To this end, we have carried out first-principles calculations for several discrete molecular units.

1. Building discrete models

The building of appropriate molecular units mimicking the situation in the solid is not an obvious task. Although some models seem reasonable from the geometric viewpoint, one must be very careful in the way of capping the atoms of the broken bonds so as to not disturb substantially the original electronic requirements of the structure. For instance, in the present systems the role of the different oxygen atoms as well as the total charge of the unit must be very carefully considered. Whereas for some models, we have been able to find the appropriate ferromagnetic and antiferromagnetic states using a variety of functionals [the hybrid B3LYP functional but also different GGA-type functionals such as PBE (Ref. 30) and BLYP (Refs. 45 and 46)], for other models we have only been able to find them using B3LYP. This clearly shows that some of these hypothetical discrete units do not provide appropriate and mutually consistent electronic environments to the metal atoms. In the present case, only the B3LYP functional, which has proven to be very robust in the study of magnetic coupling constants for many molecular systems,[38] systematically leads to convergence to the appropriate states. After careful analysis, we have found that the models shown in Figs. 4 and 5 provide appropriate discrete units to analyze the different contributions to the coupling

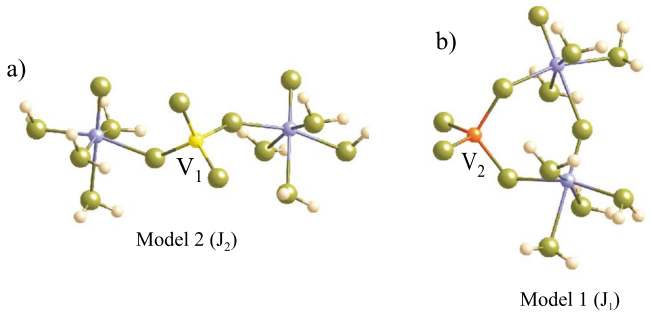

FIG. 4. (Color online) Molecular models used to analyze the magnetic coupling constants in $Sr_2V_3O_9$.

constants for $Sr_2V_3O_9$ and $Ba_2V_3O_9$, respectively.

2. Magnetostructural correlations

Let us first consider the case of $Sr_2V_3O_9$. The calculated exchange coupling constants are −42.0 K (model 2) and +35.9 K (model 1) which qualitatively mimic those calculated for the solid. Although the antiferromagnetic coupling J_2 seems to be underestimated, let us note that the same calculations with GGA-type functionals (PBE and BLYP) give values around −140 K so that the real values should be in between those of the hybrid and GGA-type functionals. Examining the ferromagnetic and antiferromagnetic states for this model, it appears that the contribution of the tetrahedral unit to the spin density is practically exclusively concentrated on the two oxygen atoms shared by the tetrahedron and the octahedra and the contribution in the V_1 vanadium atom is almost nil (see Fig. 6). Thus, we conclude that *the SSE coupling between the octahedral vanadium atoms occurs mostly through the shared oxygen atoms*.

Is it possible to correlate the different sign of the magnetic coupling constants for models 1 and 2 with the details of the structure?[24,47] The strength of the magnetic coupling illustrated in Fig. 6 will strongly depend on two factors: (i) the oxygen-oxygen distance (and thus, the deformation of the tetrahedra) and (ii) the way in which the tetrahedra bridge the

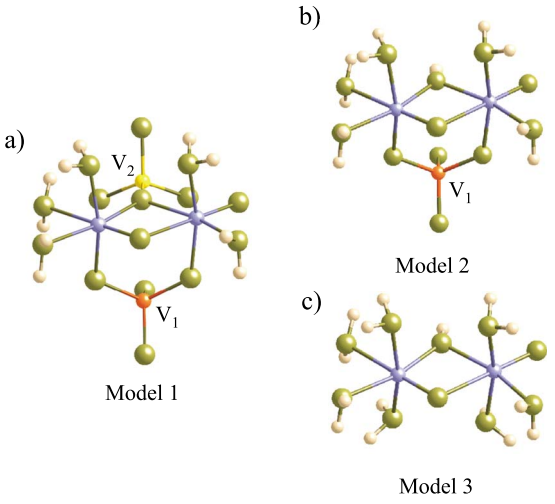

FIG. 5. (Color online) Molecular models used to analyze the magnetic coupling constants in $Ba_2V_3O_9$.

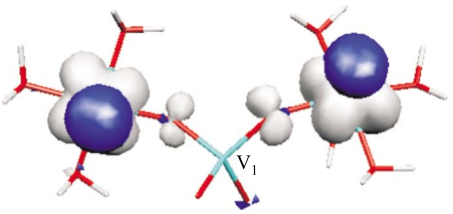

FIG. 6. (Color online) Plot of the spin density of the ferromagnetic state of model 2 for $Sr_2V_3O_9$.

two V_3 octahedral atoms. The influence of the bridging mode of a fragment or ligand on the magnetic coupling between two transition-metal atoms has been carefully studied in some dinuclear coordination compounds such as carboxylato-bridged dinuclear copper (II) systems.[48] The bridging mode imposes the overlap type between the lobes of the two oxygen orbitals implicated in the magnetic coupling and thus strongly influences it. As can be seen in Fig. 6, the bridging mode of the V_1 tetrahedra in $Sr_2V_3O_9$ (i.e., the so-called *anti-anti* mode in coordination chemistry) is such that the overlap has both π and σ components whereas in the case of the V_2 tetrahedra of model 1 (i.e., the so-called *syn-syn* mode in coordination chemistry) it is purely π (see Fig. 7). The larger overlap associated with the anti-anti mode favors the antiferromagnetic interaction. In addition, the O-O distance associated with the oxygen atoms shared by the octahedra and V_1 tetrahedra is 2.744 Å whereas it is 0.2 Å longer (2.942 Å) for the V_2 tetrahedra (i.e., those of model 1). We can thus conclude that *in terms of both distance and directionality of the oxygen orbitals, the antiferromagnetic contribution to the coupling due to the tetrahedra of* $Sr_2V_3O_9$ *increases from* V_2 *to* V_1.

Model 1 for $Sr_2V_3O_9$ is associated with a ferromagnetic coupling as it is the J_1 intrachain contribution for the $Sr_2V_3O_9$ solid. As noted in the discussion of the crystal structure, the superexchange through the shared octahedral oxygen must be weak because of local symmetry (or pseudosymmetry) reasons. As far as the V_2 tetrahedron is concerned, we note that the overlap between the shared oxygen orbitals is purely π type and the O-O distance is long. Consequently, the antiferromagnetic component of the mag-

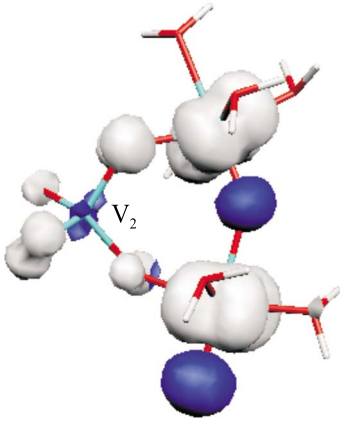

FIG. 7. (Color online) Plot of the spin density of the ferromagnetic state of model 1 for $Sr_2V_3O_9$.

netic interaction mediated by the V_2 tetrahedra must be very small. Moreover, the ferromagnetic contribution to the coupling constant, which is related to a bielectronic exchange integral, K_{ab}, where a and b are the two magnetic orbitals,[24,47] is predicted to be larger for V_2 bridging tetrahedra (syn-syn mode with V-V distances around 3.65 Å) than for V_1 bridges (anti-anti mode with V-V distances around 6.27 Å). Thus, we conclude that *the tetrahedral units bridging two octahedra in a syn-syn mode* (i.e., the V_2 tetrahedra in $Sr_2V_3O_9$) *should provide a ferromagnetic or a weak antiferromagnetic contribution to the magnetic coupling. In contrast, the coupling becomes clearly antiferromagnetic when it occurs through* VO_4 *tetrahedra bridging octahedra in a anti-anti mode* (i.e., the V_1 tetrahedra in $Sr_2V_3O_9$).

Discrete models can highlight the main features ruling the magnetic coupling but of course cannot reproduce quantitatively the coupling constants of the solid so that, at this point, one could be tempted to conclude that it is the bridging mode of the tetrahedra what imposes the nature and strength of the magnetic coupling along the two main directions of the layer. However, we should have a closer look at the possible role of the oxygen atom shared by two octahedra. Although, as discussed above, this atom should not contribute to the magnetic coupling through a *superexchange* mechanism, it could well do it through a *spin-polarization* mechanism.[24,47] This suspicion is reinforced by examination of the spin-density plots for model 1 (see Fig. 7). To have some hint on the possible implication of this oxygen atom on the magnetic coupling, we carried out calculations for a modified model 1 in which the contribution of the tetrahedron to the magnetic coupling was deleted. This was carried out by removing the central VO_2 group and saturating each of the two remaining oxygen atoms with two hydrogen atoms (i.e., by transforming them to water ligands). The calculated exchange coupling is now +52.0 K. This completely confirms that this oxygen atom is providing a substantial ferromagnetic coupling through spin polarization and, consequently, the bridging V_2 tetrahedron really must provide a weak antiferromagnetic coupling. As a matter of fact, the ferromagnetic coupling provided by this oxygen atom is not a surprise in view of some recent theoretical studies on molecular dinuclear complexes.[49,50] To summarize, our analysis suggests that in $Sr_2V_3O_9$, the V_1 tetrahedra provide a dominant antiferromagnetic interaction because of their anti-anti bridging mode, the corner-sharing oxygen atoms provide a noticeable ferromagnetic coupling along the octahedral chains through spin polarization, and the V_2 tetrahedra are almost magnetically inactive.

We can now turn to the case of $Ba_2V_3O_9$. The calculated exchange coupling constants for the three models shown in Fig. 5 are: −76.6 K (model 1), −7.2 K (model 2), and −52.8 K (model 3). Model 1 seems to describe quite well the situation in the solid since it indicates a global antiferromagnetic interaction with a coupling constant even not far from that found experimentally for the solid (−94 K). Comparison of the results obtained for model 1 and model 2 allows evaluating the role of the V_2 centered tetrahedra (yellow tetrahedra in Fig. 2). Since the net result of their removal is a strong reduction in the antiferromagnetic contribution we conclude that *the* V_2 *tetrahedra provide a substantial antiferromagnetic coupling*. If we now compare models 2 and 3, we can evaluate the role of the V_1 centered tetrahedra (orange tetrahedra in Fig. 2). Since the net result of its removal is a very noticeable increase in the antiferromagnetic coupling, we conclude that *the* V_1 *tetrahedra provide a ferromagnetic contribution to the coupling*. In model 3, we have two potential contributions to the coupling constant: (i) an antiferromagnetic superexchange contribution through the OH bridging group and (ii) a ferromagnetic contribution through the bridging oxo ligand. We have not been able to find an appropriate model converging to meaningful states to evaluate the individual contribution of the oxo ligand in this case. Suppression of any of the two bridging ligands induces a too strong perturbation of the basic electronic distribution. However, examination of the spin-density plots for the three models suggest that, as for $Sr_2V_3O_9$, the oxo ligand should provide some ferromagnetic coupling through spin polarization. Thus, let us take the −52.8 K value as a lower limit for the coupling provided by the hydroxyl group through superexchange. This, together with the −69.4 K lost from model 1 to model 2 leads to a lower limit of −122.2 K for the global contribution of the V_2 tetrahedra to the coupling. These numbers suggest that *the natural ability of the oxygen atom to participate in the superexchange coupling through its* p_z *orbital [Fig. 2(c)] is magnified by the* π*-type orbitals of the* VO_3 *tetrahedral fragment*.

As mentioned, comparison of models 2 and 3 suggest that the V_1 tetrahedra with syn-syn mode have a +45.6 K contribution to the magnetic coupling. Although this number should not be taken at its right face, especially taking into account the possible nonadditivity of magnetic contributions when two transition metals are bridged by two or more ligands,[47] this value certainly suggests that, in contrast with the situation in $Sr_2V_3O_9$, the V_1 tetrahedra in $Ba_2V_3O_9$ provide a definite ferromagnetic contribution to the coupling. In fact this is not surprising because the bielectronic exchange integral K_{ab} is larger in the case of $Ba_2V_3O_9$ because the V···V distance is considerably shorter (3.007 Å for $Ba_2V_3O_9$ vs 3.651 Å for $Sr_2V_3O_9$). In summary, *the relatively strong antiferromagnetic coupling provided by the* V_2 *tetrahedra sharing only one oxygen atom with the octahedral chain is only partially compensated by two ferromagnetic contributions from the oxygen atom nonshared with tetrahedra and the* V_1 *tetrahedra with syn-syn bridging mode*.

V. CONCLUSION

A first-principles study of the $Sr_2V_3O_9$ and $Ba_2V_3O_9$ shows that both compounds are quasi-one-dimensional spin systems and the calculated magnetic coupling constants are in very good agreement with the experimental results. $Ba_2V_3O_9$ is antiferromagnetic along the direction of the octahedral chains but $Sr_2V_3O_9$ is antiferromagnetic along the direction perpendicular to the octahedral chains. In $Sr_2V_3O_9$, the predominant coupling is antiferromagnetic and is indeed mediated by one of the two different types of tetrahedra of the structure but there is also a weaker ferromagnetic interaction along the direction of the octahedral chains, which is mediated by the corner-sharing oxygen atom. The second

type of tetrahedra (i.e., those bridging two adjacent octahedra of the chains) apparently do not play a noticeable role. The main contributor to the antiferromagnetic coupling in $Ba_2V_3O_9$ is the superexchange within the octahedral chains due to the VO_4 tetrahedra sharing one oxygen atom with the octahedra. In this case, both the tetrahedra with syn-syn bridging mode and the oxygen atoms which are nonshared with tetrahedra provide weaker ferromagnetic contributions. The effect of interchain disorder is found to have a very small influence on the coupling constants.

ACKNOWLEDGMENTS

This work was supported by DGI-Spain (Grants No. CSD2007-00041, No. FIS2009-12721-C04-03, No. CTQ2008-06670-C02-02/BQU, and No. CTQ2008-06549-C02-01/BQU), Generalitat de Catalunya (2009 SGR 1459 and 2009 SGR 462), XRQTC, and by grants for computer time from CESCA. A.R.-F. acknowledges support through the Ramón y Cajal program (DGI-Spain).

[1] H. G. von Schnering, Yu. Grin, M. Kaupp, R. K. Kremer, O. Jepsen, T. Chatterji, and M. Weiden, Z. Kristallogr. **213**, 243 (1998).
[2] H. Kobayashi, Bull. Chem. Soc. Jpn. **52**, 1315 (1979).
[3] M. Isobe and Y. Ueda, J. Phys. Soc. Jpn. **65**, 1178 (1996).
[4] T. Ohama, H. Yasuoka, M. Isobe, and Y. Ueda, Phys. Rev. B **59**, 3299 (1999).
[5] H. Yamada and Y. Ueda, J. Phys. Soc. Jpn. **68**, 2735 (1999).
[6] T. Yamauchi, Y. Ueda, and N. Mori, Phys. Rev. Lett. **89**, 057002 (2002).
[7] P. Millet, J. Y. Henri, F. Mila, and J. Galy, J. Solid State Chem. **147**, 676 (1999).
[8] J. L. Gavilano, D. Rau, S. Mushkolaj, H. R. Ott, P. Millet, and F. Mila, Phys. Rev. Lett. **90**, 167202 (2003).
[9] J. L. Gavilano, E. Felder, D. Rau, H. R. Ott, P. Millet, F. Mila, T. Cichorek, and A. C. Mota, Phys. Rev. B **72**, 064431 (2005).
[10] A. Rodríguez-Fortea, M. Llunell, P. Alemany, and E. Canadell, Inorg. Chem. **48**, 5779 (2009).
[11] J. Feldmann and Hk. Müller-Buschbaum, Z. Naturforsch. B **50**, 43 (1995).
[12] O. Mentre, A.-C. Dhaussy, F. Abraham, and H. Steinfink, J. Solid State Chem. **140**, 417 (1998).
[13] E. E. Kaul, H. Rosner, V. Yushankhai, J. Sichelschmidt, R. V. Shpanchenko, and C. Geibel, Phys. Rev. B **67**, 174417 (2003).
[14] M. Isobe, Y. Ueda, Y. Oka, and T. Yao, J. Solid State Chem. **145**, 361 (1999).
[15] P. Millet, J.-Y. Henry, and J. Galy, Acta Crystallogr., Sect. C: Cryst. Struct. Commun. **55**, 276 (1999).
[16] F. Duc, P. Millet, S. Ravy, A. Thiollet, F. Chabre, A. M. Ghorayeb, F. Mila, and A. Stepanov, Phys. Rev. B **69**, 094102 (2004).
[17] H.-J. Koo and M.-H. Whangbo, Solid State Sci. **9**, 824 (2007).
[18] A.-C. Dhaussy, F. Abraham, O. Mentré, and H. Steifink, J. Solid State Chem. **126**, 328 (1996).
[19] O. Mentré, A. C. Dhaussy, F. Abraham, E. Suard, and H. Steinfink, Chem. Mater. **11**, 2408 (1999).
[20] V. A. Ivanshin, V. Yushankhai, J. Sichelschmidt, D. V. Zakharov, E. E. Kaul, and C. Geibel, Phys. Rev. B **68**, 064404 (2003).
[21] V. A. Ivanshin, V. Yushankhai, J. Sichelschmidt, D. V. Zakharov, E. E. Kaul, and C. Geibel, J. Magn. Magn. Mater. **272-276**, 960 (2004).
[22] A. A. Gippius, E. N. Morozova, R. V. Spanchenko, E. E. Kaul, C. Geibel, A. Rabis, M. Baenitz, and F. Steglich, J. Magn. Magn. Mater. **272-276**, 956 (2004).
[23] B. Schmidt, V. Yushankhai, L. Siurakshina, and P. Thalmeier, Eur. Phys. J. B **32**, 43 (2003).
[24] P. J. Hay, J. Thibeault, and R. Hoffmann, J. Am. Chem. Soc. **97**, 4884 (1975).
[25] P. Hohenberg and W. Kohn, Phys. Rev. **136**, B864 (1964).
[26] W. Kohn and L. J. Sham, Phys. Rev. **140**, A1133 (1965).
[27] J. M. Soler, E. Artacho, J. Gale, A. García, J. Junquera, P. Ordejón, and D. Sánchez-Portal, J. Phys.: Condens. Matter **14**, 2745 (2002).
[28] For more information on the SIESTA code visit: http://www.uam.es/siesta/
[29] For a review on applications of the SIESTA approach in materials science, see D. Sánchez-Portal, P. Ordejón, and E. Canadell, Structure and Bonding (Berlin) **113**, 103 (2004).
[30] J. P. Perdew, K. Burke, and M. Ernzerhof, Phys. Rev. Lett. **77**, 3865 (1996).
[31] N. Troullier and J. L. Martins, Phys. Rev. B **43**, 1993 (1991).
[32] L. Kleinman and D. M. Bylander, Phys. Rev. Lett. **48**, 1425 (1982).
[33] S. G. Louie, S. Froyen, and M. L. Cohen, Phys. Rev. B **26**, 1738 (1982).
[34] E. Artacho, D. Sánchez-Portal, P. Ordejón, A. García, and J. M. Soler, Phys. Status Solidi B **215**, 809 (1999).
[35] H. J. Monkhorst and J. D. Park, Phys. Rev. B **13**, 5188 (1976).
[36] E. Ruiz, M. Llunell, and P. Alemany, J. Solid State Chem. **176**, 400 (2003).
[37] A. D. Becke, J. Chem. Phys. **98**, 5648 (1993).
[38] E. Ruiz, Structure and Bonding (Berlin) **113**, 71 (2004).
[39] E. Ruiz, P. Alemany, S. Alvarez, and J. Cano, J. Am. Chem. Soc. **119**, 1297 (1997).
[40] A. Rodríguez-Fortea, P. Alemany, S. Alvarez, and E. Ruiz, Eur. J. Inorg. Chem. **2004**, 143.
[41] A. Schäfer, C. Huber, and R. Ahlrichs, J. Chem. Phys. **100**, 5829 (1994).
[42] M. J. Frisch *et al.*, GAUSSIAN 03, revisions B.4 and C.1; Gaussian Inc.: Pittsburgh, PA, 2003.
[43] E. Ruiz, J. Cano, S. Alvarez, and P. Alemany, J. Comput. Chem. **20**, 1391 (1999).
[44] J. Feldmann and Hk. Müller-Buschbaum, Z. Naturforsch. B **51**, 489 (1996).
[45] A. D. Becke, Phys. Rev. A **38**, 3098 (1988).
[46] C. Lee, W. Yang, and R. G. Parr, Phys. Rev. B **37**, 785 (1988).
[47] O. Kahn, *Molecular Magnetism* (VCH, New York, 1993).
[48] A. Rodríguez-Fortea, P. Alemany, S. Alvarez, and E. Ruiz, Chem.-Eur. J. **7**, 627 (2001).
[49] E. Ruiz, S. Alvarez, and P. Alemany, Chem. Commun. (Cambridge) **1998**, 2767.
[50] E. Ruiz, C. de Graaf, P. Alemany, and S. Alvarez, J. Phys. Chem. A **106**, 4938 (2002).